The Plant Cell, Vol. 17, 1764–1776, June 2005, www.plantcell.org

KATAMARI1/MURUS3 Is a Novel Golgi Membrane Protein That Is Required for Endomembrane Organization in Arabidopsis [W]

Kentaro Tamura,[a] Tomoo Shimada,[a] Maki Kondo,[b] Mikio Nishimura,[b] and Ikuko Hara-Nishimura[a,1]

[a] Department of Botany, Graduate School of Science, Kyoto University, Kyoto 606-8502, Japan
[b] Department of Cell Biology, National Institute for Basic Biology, Okazaki 444-8585, Japan

In plant cells, unlike animal and yeast cells, endomembrane dynamics appear to depend more on actin filaments than on microtubules. However, the molecular mechanisms of endomembrane–actin filament interactions are unknown. In this study, we isolated and characterized an *Arabidopsis thaliana* mutant, *katamari1* (*kam1*), which has a defect in the organization of endomembranes and actin filaments. The *kam1* plants form abnormally large aggregates that consist of endoplasmic reticulum with actin filaments in the perinuclear region within the cells and are defective in normal cell elongation. Map-based cloning revealed that the *KAM1* gene is allelic to the *MUR3* gene. We demonstrate that the KAM1/MUR3 protein is a type II membrane protein composed of a short cytosolic N-terminal domain and a transmembrane domain followed by a large lumenal domain and is localized specifically on Golgi membranes. We further show that actin filaments interact with Golgi stacks via KAM1/MUR3 to maintain the proper organization of endomembranes. Our results provide functional evidence that KAM1/MUR3 is a novel component of the Golgi-mediated organization of actin functioning in proper endomembrane organization and cell elongation.

INTRODUCTION

The endomembrane system is composed of the endoplasmic reticulum (ER), Golgi stacks, endosomes, and vacuoles in plant cells. Membrane traffic between these endomembranes is important for plant cell division, growth, differentiation, and function during development. The ER is an essential organelle for protein assembly and lipid biosynthesis and acts as the beginning of the secretory pathway (Vitale and Denecke, 1999). The ER usually consists of a polygonal meshwork of membrane tubules and variously shaped sheet-like cisternae (Grabski et al., 1993; Boevink et al., 1996). These structures are interconnected with one another and with the continuous membrane of the outer nuclear envelope (Herman et al., 1990; Boevink et al., 1996). Unlike mammalian cells, in which Golgi stacks are practically immobile and condensed in a limited perinuclear region, plant cells contain a large number of Golgi stacks throughout the cytoplasm. Green fluorescent protein (GFP) fusions have allowed the visualization of the Golgi stacks in vivo and revealed that each stack is highly mobile, moving around the ER and actin filaments driven by myosin motors (Boevink et al., 1998; Nebenfuhr et al., 1999). Vacuoles, which are the most prominent compartment in the plant cell, also have a dynamic and complex membrane structure. Studies using a vacuolar membrane–targeted GFP found that spherical structures (bulbs) consisting of a double membrane were often observed within the lumen of vacuoles and were connected with the vacuolar membrane (Saito et al., 2002; Uemura et al., 2002). These bulbs were observed to move around within or along the outline of the membrane, mediated by the actin filaments but not by the microtubules (Uemura et al., 2002).

The structural and functional maintenance of endomembranes is also important for various aspects of plant development and signal transduction (Surpin and Raikhel, 2004). The *vacuoleless* (*vcl1*) mutant of *Arabidopsis thaliana*, which has no obvious vacuoles, does not survive beyond the torpedo stage of embryonic development (Rojo et al., 2001). Because Arabidopsis VCL1 is a homolog of yeast Vacuolar Protein-Sorting 16, which regulates the homotypic fusion of vacuoles and the docking of vesicles (Sato et al., 2000), the *vcl1* mutant may have defects in the very early stages of vacuole biogenesis. Some *shoot gravitropism* (*sgr*) mutants of Arabidopsis have abnormal vacuolar and vesicular structures in several tissues, including the endodermis, in which gravity is sensed by sedimentable amyloplasts (Kato et al., 2002; Morita et al., 2002; Yano et al., 2003). Two *SGR* genes encode protein components of vesicle trafficking, and another *SGR* gene encodes a protein that regulates vacuolar membrane structure.

Two cytoskeleton systems (i.e., actin filaments and microtubules) are indispensable for the intracellular positioning and dynamic movement of organelles. In plant cells, the dynamics of endomembranes appear to depend more on actin filaments than on microtubules. Thus, it is believed that plant cells develop unique mechanisms for endomembrane organization that depend on actin filaments (Boevink et al., 1998; Brandizzi et al., 2002). To elucidate the molecular mechanisms that regulate endomembrane organization in plants, we screened Arabidopsis seedlings for mutants that have a defect in endomembrane

[1] To whom correspondence should be addressed. E-mail ihnishi@gr.bot.kyoto-u.ac.jp; fax 81-75-753-4142.
The author responsible for distribution of materials integral to the findings presented in this article in accordance with the policy described in the Instructions for Authors (www.plantcell.org) is: Ikuko Hara-Nishimura (ihnishi@gr.bot.kyoto-u.ac.jp).
[W] Online version contains Web-only data.
Article, publication date, and citation information can be found at www.plantcell.org/cgi/doi/10.1105/tpc.105.031930.

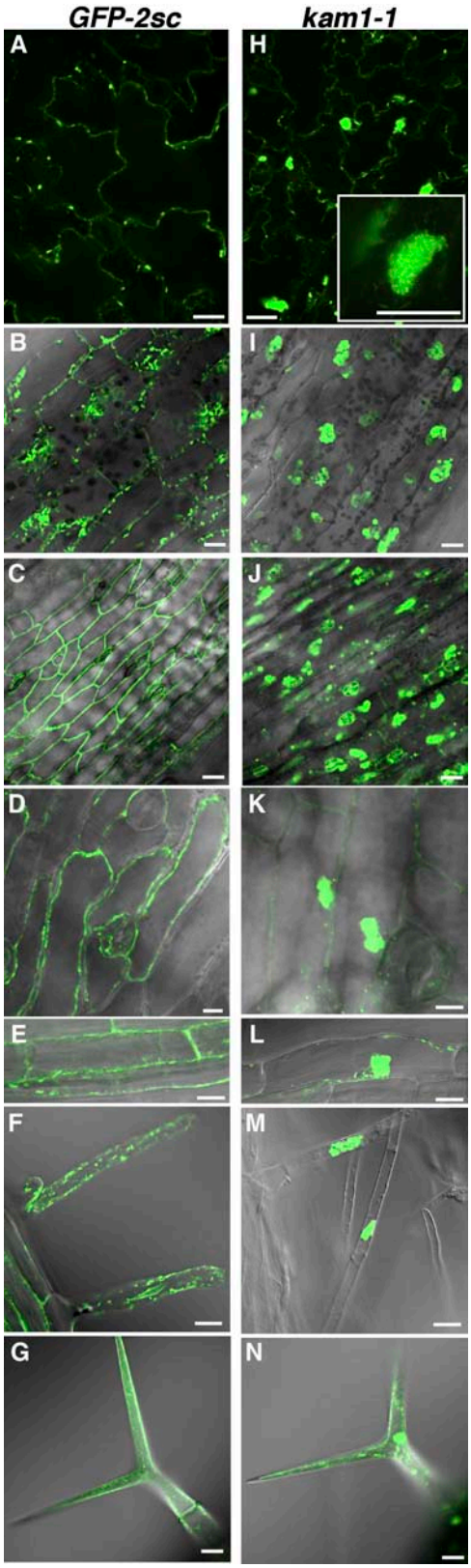

Figure 1. Disorganization and Aggregation of Endomembranes in Different Organs of the Isolated Arabidopsis Mutant *kam1*.

organization. Here, we report the isolation and characterization of a mutant (termed *katamari1* [*kam1*]) in which the endomembranes formed large aggregates. We provide evidence that KAM1 mediates the actin organization that contributes to endomembrane organization and cell elongation.

RESULTS

The *kam1* Mutant, Which Has a Defect in Endomembrane Organization, Includes Abnormal Aggregates of Various Organelles in the Perinuclear Region of the Cells

To isolate Arabidopsis mutants that have an abnormal endomembrane structure within the cells, we used a transgenic Arabidopsis, *GFP-2sc*, which expresses vacuole-targeted GFP-2SC. Previously, we reported the light-dependent disappearance of GFP fluorescence in the vacuoles (Tamura et al., 2003). Light-grown *GFP-2sc* does not exhibit fluoresced vacuoles but maintains GFP fluorescence in entire endomembranes, including ER network structures and dot-like structures of the Golgi complex (Tamura et al., 2003) (Figures 1A to 1G; see Supplemental Video 1 online). In this study, all fluorescent images were taken from light-grown plants.

GFP-2sc seeds were mutagenized, and 669 M2 lines were obtained. Of ~12,000 M2 seedlings examined with the fluorescence microscope, we isolated a mutant whose endomembrane formed large aggregates and designated the mutant *kam1* (for *katamari1*), after the Japanese word for aggregate. The aggregates (~10 μm) were found in most of the cells of cotyledons (Figure 1H), hypocotyls (Figure 1I), and flower stalks (Figure 1J); they were also found in some cells of siliques (Figure 1K), roots (Figure 1L), root hairs (Figure 1M), and trichomes (Figure 1N). A higher magnification of a fluorescent image showed that the aggregates were composed of many small particles (Figure 1H, inset). Small aggregates of endomembranes that moved on the ER network were also observed on the surface of leaf cells (see Supplemental Video 2 online). These observations imply that the endomembranes are fragmented and/or deformed.

To identify the components of the aggregates, we visualized various organelles in leaf epidermal cells from 15-d-old seedlings

Median planes of various cells of transgenic Arabidopsis (*GFP-2sc*; left panels) and the isolated mutant (*kam1-1*; right panels) were inspected with a confocal laser scanning microscope and a differential interference contrast (DIC) microscope. Bars = 10 μm.

(A) and **(H)** GFP-fluorescent images of 7-d-old cotyledons. The inset in **(H)** shows a higher magnification of a GFP-fluoresced aggregate.

(B) and **(I)** Merged images of GFP and DIC of hypocotyls of 15-d-old plants.

(C) and **(J)** Merged images of GFP and DIC of flower stalks of 6-week-old plants.

(D) and **(K)** Merged images of GFP and DIC of siliques of 6-week-old plants.

(E) and **(L)** Merged images of GFP and DIC of roots of 15-d-old plants.

(F) and **(M)** Merged images of GFP and DIC of root hairs of 15-d-old plants.

(G) and **(N)** Merged images of GFP and DIC of trichomes of 15-d-old plants.

of *GFP-2sc* (Figures 2A to 2E) and *kam1-1* (Figures 2F to 2J) by transient expression of monomeric red fluorescent protein (mRFP)–tagged marker proteins (Campbell et al., 2002), FM4-64 staining, and 4′,6-diamidino-2-phenylindole (DAPI) staining. Most of the RFP-fluorescent ERs were completely merged with the GFP-fluorescent aggregates, causing the aggregates to become yellow fluorescent (Figure 2F). Some of the RFP-fluorescent Golgi stacks were engulfed in the aggregates (Figure 2G). Some of the RFP-fluorescent peroxisomes were detected as red fluorescent particles in the aggregates (Figure 2H). Most of the FM4-64–stained endosomes were detected as red fluorescent small particles and their assembly, which were found in the green fluorescent aggregates (Figure 2I). These results suggested that the ER is specifically aggregated, whereas the Golgi, peroxisomes, and endosomes are nonspecifically engulfed in the aggregates in *kam1* cells. DAPI-stained nuclei were close to the GFP-fluorescent aggregates (Figure 2J), suggesting that the aggregates are located in the perinuclear region.

Electron microscopic analysis showed that the epidermal cells of wild-type roots were occupied by a large central vacuole surrounded by a cytosol (Figure 3A). On the contrary, epidermal cells of *kam1-1* roots had a cytoplasmic aggregate abnormally at the center of the cell (Figure 3B). Higher magnification (Figure 3C) revealed that the cytoplasmic aggregate contained many fragmented vacuoles and a nucleus. These results suggest that the aggregates, which are composed of various organelles, including nuclei, are found in cells of different organs in *kam1-1*.

KAM1 Is Allelic to *MUR3*, Encoding a Protein That Has an Exostosin-Like Domain

To identify the *KAM1* gene, we used a map-based cloning approach with codominant cleaved amplified polymorphic sequence markers (Konieczny and Ausubel, 1993) and simple sequence length polymorphism markers (Bell and Ecker, 1994) and found that *KAM1* is located on chromosome 2 between markers PHYB and mi421. Further mapping using 450 F2 plants that exhibited the phenotype conferred by *kam1* and DNA sequencing showed a single base pair mutation from C to T in the At2g20370 gene of *kam1-1*, which might cause a nonsense mutation from CAA (Gln-62) to TAA (stop codon) (Figure 4A).

To confirm that the mutation in the At2g20370 gene is responsible for the phenotype conferred by *kam1*, we analyzed knockout mutants of the At2g20370 gene from the Salk T-DNA insertion line collections. We isolated two lines in which T-DNA was inserted into the At2g20370 coding region and named these mutants (salk_127057 and salk_141953) *kam1-2* and *kam1-3*, respectively (Figure 4A). To visualize the endomembranes, a vacuole-targeted GFP, SP-GFP-2SC, was transiently expressed in epidermal cells of rosette leaves of each *kam1* allele by particle bombardment. Figure 4B (top row) shows the aggregates of endomembranes in the *kam1-2* and *kam1-3* cells, as seen in the *kam1-1* cells. In addition, we confirmed that constitutive expression of KAM1-mRFP (see Figure 6B) rescued the phenotype conferred by *kam1* (data not shown). These results indicate that *KAM1* is the At2g20370 gene.

The *KAM1* gene encodes a polypeptide sequence of 619 amino acids with a single putative transmembrane domain (Figure 4A).

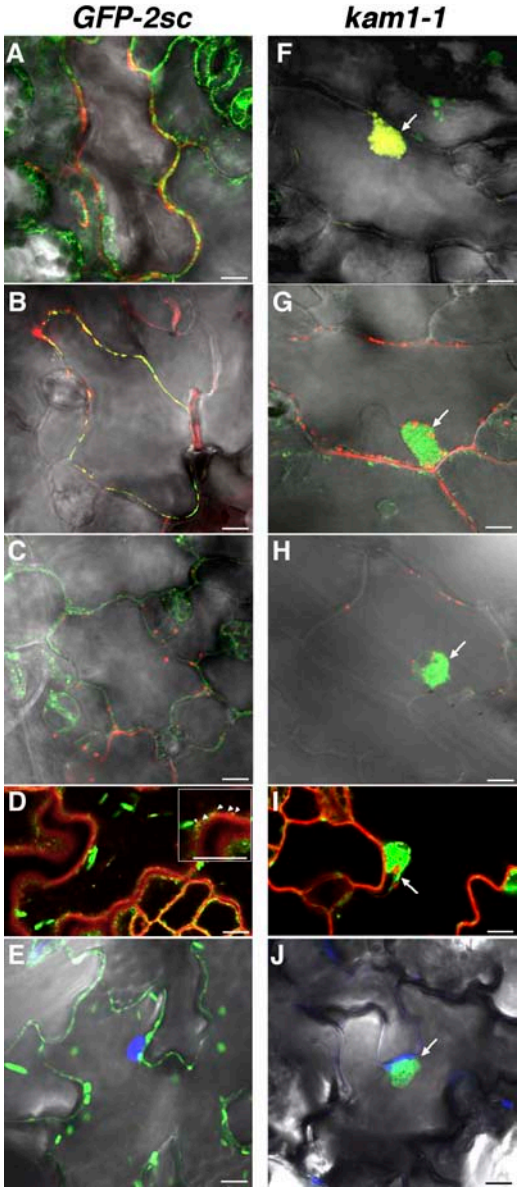

Figure 2. Aggregates in Epidermal Cells of *kam1-1* Contain Various Organelles.

Various organelles were visualized in epidermal cells from 15-d-old cotyledons of *GFP-2sc* (left panels) and *kam1-1* (right panels) by transient expression of mRFP-tagged organelle markers, FM4-64 staining, and DAPI staining and then inspected with a confocal laser scanning microscope and a differential interference contrast microscope. Arrows indicate GFP-fluoresced aggregate. Bars = 10 μm.

(A) and **(F)** Merged images of a single cell expressing ER-targeted mRFP and GFP-2SC.

(B) and **(G)** Merged images of a single cell expressing Golgi-targeted mRFP and GFP-2SC.

(C) and **(H)** Merged images of a single cell expressing peroxisome-targeted mRFP and GFP-2SC.

(D) and **(I)** FM4-64 staining of plasma membrane and endosomes (red). The inset shows a higher magnification of endosomes (arrowheads).

(E) and **(J)** DAPI staining of nuclei (blue).

Immunoblot analysis with the anti-KAM1LD antibody showed that the 84-kD protein was accumulated in *GFP-2sc* but not in *kam1-1*, *kam1-2*, or *kam1-3* (Figure 4C). KAM1 had an exostosin-like domain (Solomon, 1964) (Figure 4A, green box). Exostosins act as glycosyltransferases, which catalyze the formation of heparan sulfate, an extracellular glycosaminoglycan in animal cells (Esko and Selleck, 2002). The Arabidopsis mutants *mur3-1* and *mur3-2*, which have a missense mutation in the At2g20370 gene, lacked glycosyltransferase activity (Madson et al., 2003). To determine whether a deficiency of glycosyltransferase activity in KAM1 is responsible for the defect in endomembrane organization in *kam1*, we examined endomembrane organization in *mur3-1* and *mur3-2*. The 84-kD immunopositive protein was accumulated in *mur3-1* and *mur3-2* as in *GFP-2sc* (Figure 4C). We expressed the vacuole-targeted GFP in *mur3-1* and *mur3-2* leaves and inspected the GFP-fluorescent endomembranes. Both mutants exhibited normal endomembrane organization in the cells, like wild-type plants (Figure 4B, bottom row). This result indicates that glycosyltransferase activity is not involved in the organization of the endomembranes.

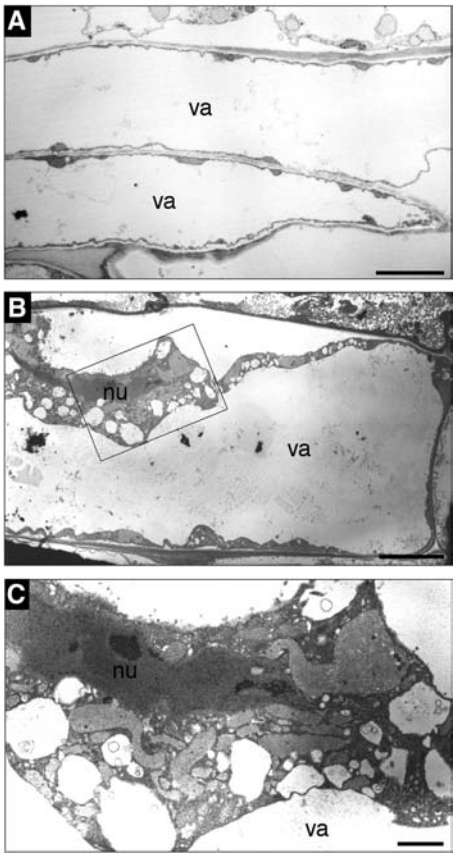

Figure 3. *kam1-1* Root Cells Form an Abnormal Aggregate of Cytoplasm in the Perinuclear Region.

(A) and **(B)** Electron micrographs of root epidermal cells of the wild type **(A)** and *kam1-1* **(B)**. Bars = 5 μm **(A)** and 10 μm **(B)**.
(C) Higher magnification of the boxed area in **(B)**. Bar = 2 μm.
nu, nucleus; va, vacuole.

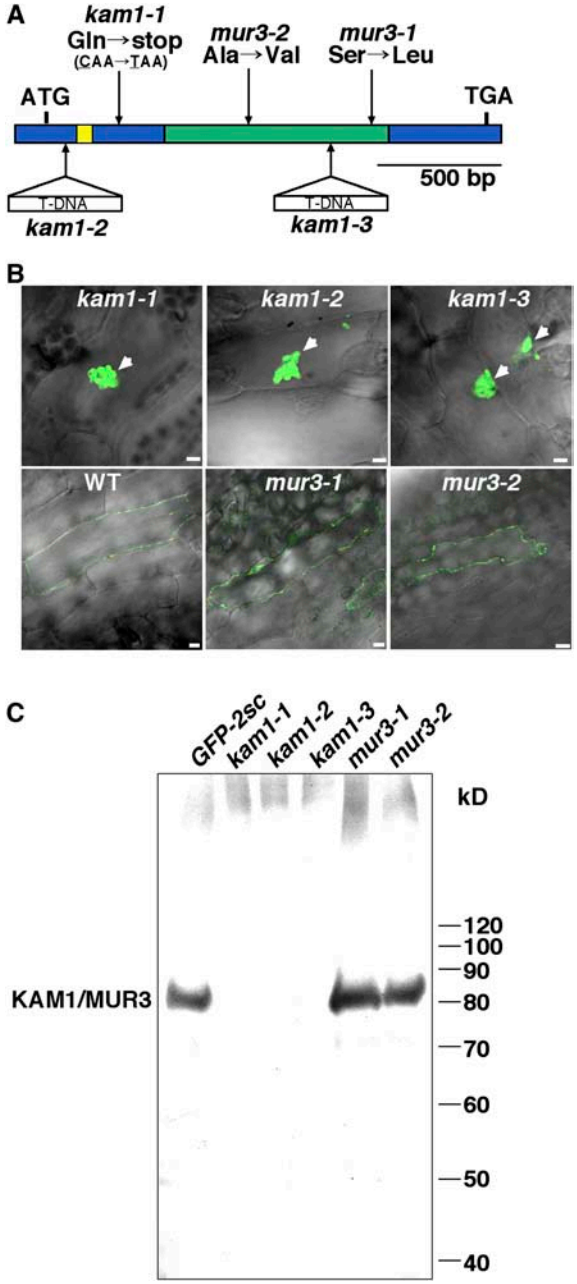

Figure 4. Analysis of *kam1* Mutant Alleles.

(A) Structure of the *KAM1/MUR3* gene, which is an intronless gene. The site of each mutation of *kam1-1*, *mur3-1*, and *mur3-2* is indicated. The site of each T-DNA insertion of *kam1-2* and *kam1-3* is indicated as well. The yellow box indicates the coding region for a putative transmembrane domain, and the green box indicates the coding region for an exostosin-like domain.
(B) Structure of endomembranes in each *kam1* allele. To visualize endomembrane structures, a chimeric gene encoding SP-GFP-2SC, a vacuole-targeted GFP, was transiently expressed after particle bombardment of rosette leaf epidermal cells of each *kam1* allele. Arrowheads indicate the aggregates of endomembrane. Bars = 10 μm.
(C) Immunoblot analysis of *kam1* alleles. The same protein amounts of membrane fraction isolated from each *kam1* allele were subjected to immunoblot analysis with anti-KAM1LD. Molecular masses are given at right.

KAM1/MUR3 Is a Type II Integral Membrane Protein That Localizes on the Golgi Stacks

A hydropathy plot of KAM1/MUR3 (Figure 5A) suggests that a transmembrane domain (bar) is located in the N-terminal region. KAM1/MUR3 was extracted from microsomes of wild-type seedlings by detergent (Triton X-100) but not by high salt (NaCl) or alkaline pH (pH 11) (Figure 5B). This profile was the same as that of an integral membrane protein, AtVSR (for *Arabidopsis thaliana* vacuolar sorting receptor) (Shimada et al., 2003). This result indicates that KAM1/MUR3 is an integral membrane protein.

To determine the membrane topology of KAM1/MUR3, we used transgenic Arabidopsis plants, which overexpress the KAM1-mRFP fusion in the *kam1-1* background. The phenotypes conferred by *kam1* were fully complemented in the transgenic plants, suggesting that KAM1-mRFP has activity for endomembrane organization, like endogenous KAM1/MUR3. Microsomes isolated from the transgenic plants were incubated with proteinase K either in the presence or the absence of detergent. Subsequently, the sensitivity of KAM1/MUR3 was evaluated by immunoblot analysis with anti-KAM1LD antibody, which was raised against the C-terminal domain of KAM1/MUR3. KAM1-mRFP became sensitive to protease digestion only when the microsomes were solubilized with detergent (Figure 5C, lane 4), suggesting that the epitope is exposed to the lumen. These results, together with the hydropathy analysis, indicate that KAM1/MUR3 has a type II topology, with a short N terminus exposed to the cytosol, a single transmembrane-spanning domain, and a C terminus inside the lumen.

In sucrose density gradient fractions of a homogenate of Arabidopsis seedlings, KAM1/MUR3 cosedimented with a Golgi marker, RGP1 (Dhugga et al., 1997), but not with a prevacuolar compartment/*trans*-Golgi network marker, AtVSR, or a ER marker, BiP (Figure 6A). This finding suggests that KAM1/MUR3 is localized on the Golgi stack. To visualize the intracellular localization of KAM1/MUR3, we constructed chimeric genes encoding modified mRFPs. KAM1-mRFP was composed of the full length of KAM1/MUR3 followed by mRFP, whereas KAM1ΔC-mRFP was composed of the C-terminal-truncated form of KAM1/MUR3 (120 amino acids) followed by mRFP (Figure 6B). Each fusion protein was transiently expressed in protoplasts prepared from Arabidopsis suspension-cultured cells. These modified mRFPs were completely merged with a GFP-fluorescent Golgi marker (GFP-AVP2) (Mitsuda et al., 2001) (Figure 6C). These results indicate that KAM1/MUR3 localizes on the Golgi stacks and that its N-terminal portion (120 amino acids) is sufficient for Golgi targeting.

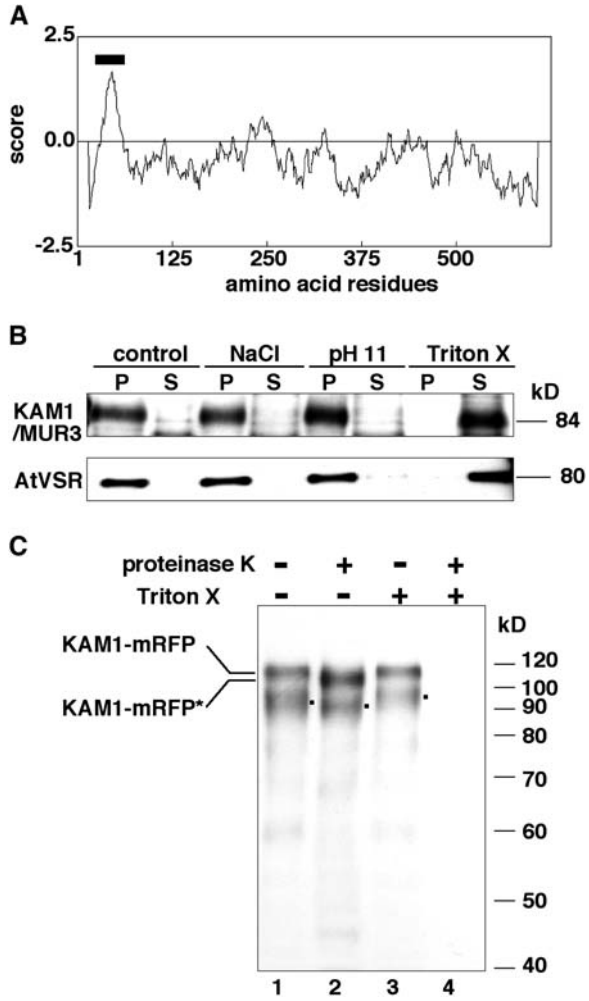

Figure 5. KAM1/MUR3 Is a Type II Membrane Protein.

(A) Hydropathy plot of KAM1/MUR3 as calculated according to Kyte and Doolittle (1982). The hydrophobic region is shown as a gray bar.

(B) Microsomal fractions from wild-type seedlings were resuspended in control buffer (control; 100 mM Hepes-KOH, pH 7.5), high-salt buffer (NaCl; 1 M NaCl and 100 mM Hepes-KOH, pH 7.5), alkaline buffer (pH 11; Na_2CO_3, pH 11), and Triton X-100 buffer (Triton X; 1% [v/v] Triton X-100 and 100 mM Hepes-KOH, pH 7.5). These suspensions were ultracentrifuged to obtain supernatant (S) and pellet (P) fractions. Each fraction was subjected to immunoblot analysis with anti-KAM1LD and anti-AtVSR antibodies. Molecular masses are given at right.

(C) Microsomal fractions from transgenic Arabidopsis seedlings, which express the KAM1-mRFP fusion, were incubated in the presence (+) or absence (−) of Triton X-100 and proteinase K and then subjected to immunoblot analysis with anti-KAM1LD antibody. KAM1-mRFP, full-length KAM1-mRFP; KAM1-mRFP*, truncated form of KAM1-mRFP. Dots indicate degraded products or nonspecific bands. Molecular masses are given at right.

KAM1/MUR3 Interacts with Actin, Whose Filaments Are Necessary for the Proper Endomembrane Organization in Cells

It is well known that the cytoskeleton is involved in the intracellular positioning and movement of organelles. To investigate how the cytoskeleton contributes to the maintenance of endomembranes, we examined the effect of cytoskeleton-disordering reagents on the endomembranes of *GFP-2sc* seedlings. Latrunculin B, which depolymerizes actin filaments, disordered the endomembranes in epidermal cells of cotyledons (Figures 7A and 7B). The network structure of the cortical ER was completely

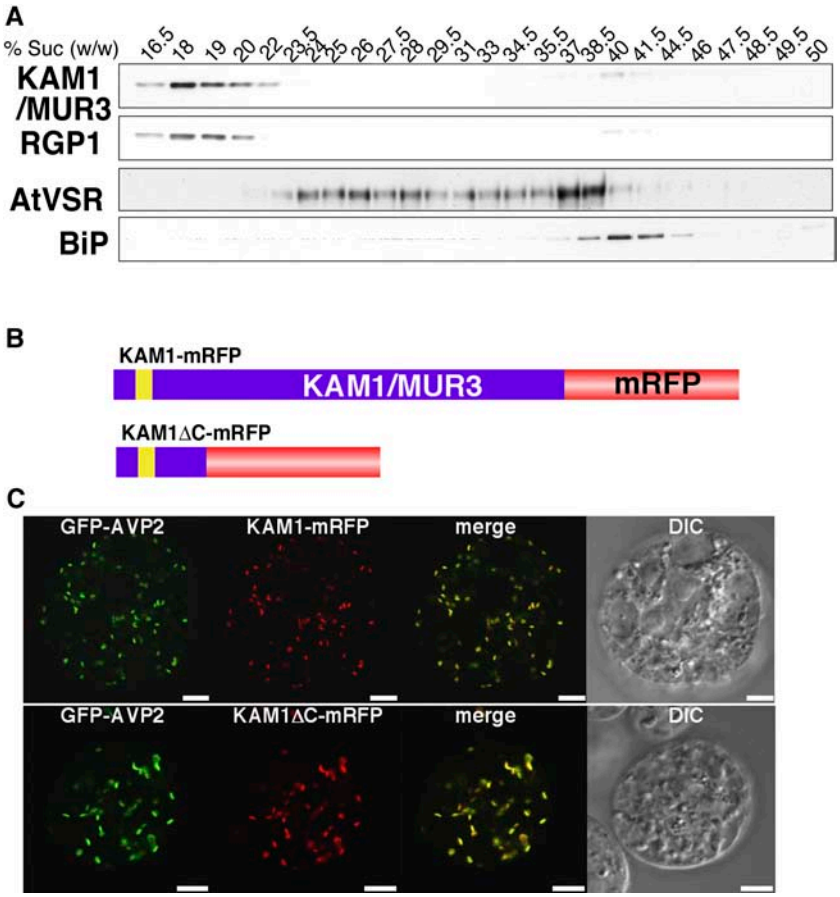

Figure 6. KAM1/MUR3 Localizes on the Golgi Stacks.

(A) Microsomal fractions from Arabidopsis seedlings were further fractionated on a sucrose density gradient (10 to 50%, w/w). The fractions obtained were numbered from top to bottom of the gradient. Each fraction was subjected to immunoblot analysis with anti-KAM1LD and specific antibodies for various organelle markers: anti-RGP1 (a Golgi marker), anti-AtVSR (a *trans*-Golgi network and prevacuolar compartment marker), and anti-BiP (an ER marker). The sucrose concentration of each fraction measured is given at top.

(B) Two mRFP-tagged KAM1/MUR3 fusion proteins. mRFP was fused to full-length KAM1/MUR3 (619 amino acids) and the C-terminal truncated form of KAM1/MUR3 (120 amino acids). The fusion proteins were designated KAM1-mRFP and KAM1ΔC-mRFP, respectively. Yellow boxes indicate a putative transmembrane domain of KAM1/MUR3.

(C) A Golgi-localized GFP fusion (GFP-AVP2) was coexpressed with KAM1-mRFP (top row) and KAM1ΔC-mRFP (bottom row) transiently in protoplasts of Arabidopsis cultured cells. The cells were inspected with a confocal laser scanning microscope and a differential interference contrast (DIC) microscope. Bars = 5 μm.

destroyed, and blobs of the endomembranes were formed on the surface of latrunculin B–treated cells (Figure 7A). Aggregates of endomembranes were found in the perinuclear region of the treated cells (Figure 7B), as in *kam1* cells. On the contrary, neither of two microtubule-disordering reagents (nocodazol and colchicine) had any effect on the structure of the endomembranes (Figures 7D and 7E). We also found that the latrunculin B–induced aggregates were perfectly colocalized with the mRFP-tagged ER marker (Figure 7C). These results suggest that intact actin filaments, but not microtubules, are necessary for the maintenance of endomembrane structures.

Treatment with the actin-depolymerizing reagent caused *GFP-2sc* cells to develop a *kam1*-like phenotype. This implies that actin is disorganized in the phenotype conferred by *kam1*. Staining with phalloidin revealed that some of actin filaments coaggregated with the endomembranes in *kam1-1* cotyledon cells (Figure 8A, right panels, arrows), whereas no aggregates of actin were found in *GFP-2sc* cells (Figure 8A, left panels). To confirm the organization of actin filaments in living cells, we transiently expressed the *ABD2-GFP* construct, which encodes an actin binding domain of fimbrin protein followed by GFP (Wang et al., 2004), in the wild type (Figure 8B, left panels) and *kam1-2*, which has no GFP (Figure 8B, right panels). The actin filaments were aggregated and the cortical network partially disappeared in *kam1-2*. However, a few intact actin filaments were still found in *kam1* cells (Figures 8A and 8B, right panels),

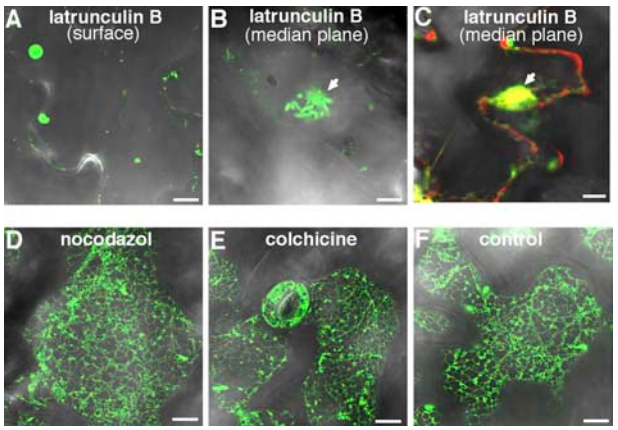

Figure 7. Intact Actin Filaments Are Required for the Organization of Endomembranes within the Cells.

Seven-day-old seedlings of *GFP-2sc* were incubated in MS medium containing 15 μM latrunculin B (**[A]** to **[C]**), 10 μM nocodazol **(D)**, and 1 mM colchicine **(E)** for 12 h. The seedlings were also incubated with 1% DMSO as a control **(F)**. After treatment, surface planes (**[A]** and **[D]** to **[F]**) and median planes (**[B]** and **[C]**) of epidermal cells of the cotyledons were inspected with a confocal laser scanning microscope and a differential interference contrast microscope. The ER **(C)** was visualized by transient expression of mRFP-tagged organelle markers (red). Arrows indicate a GFP-fluoresced aggregate. Bars = 10 μm.

suggesting that the mutant phenotype is not completely equivalent to the result of actin depolymerization.

These results raise the possibility that KAM1/MUR3 interacts with actin and regulates the proper distribution of actin filaments in wild-type plants. To investigate this possibility, we immunoprecipitated detergent-solubilized extracts from Arabidopsis cultured cells with both anti-KAM1LD and anti-KAM1CT antibodies. The immunoprecipitates were subjected to immunoblot analysis with anti-KAM1LD or anti-actin antibodies. The results clearly show that KAM1/MUR3 coimmunoprecipitated with actin (Figure 8C). On the contrary, actin did not precipitate in the control experiments with each preimmune serum (Figure 8C) or anti-BiP and anti-AtVSR1 antibodies (see Supplemental Figure 1 online). This result suggests that KAM1/MUR3 interacts with actin within the cells.

kam1 Has a Defect in Cell Elongation

kam1-1 showed a dwarf phenotype at different developmental stages (Figure 9). The *kam1-1* seedlings were significantly smaller than the *GFP-2sc* seedlings (Figure 9A). The *kam1-1* plants had wrinkled leaves and short petioles (Figure 9B) and exhibited dwarf stature (Figure 9C). When grown in the dark, the length of the *kam1-1* hypocotyl was only one-third that of the *GFP-2sc* hypocotyl (Figure 9D). These phenotypes were also observed in *kam1-2* and *kam1-3* plants but not in *mur3-1* or *mur3-2* plants (data not shown). The *kam1-1* cells in hypocotyls were significantly smaller and fatter than *GFP-2sc* cells and exhibited abnormal shape (Figures 9E and 9F). On the contrary, there were no differences in the number of epidermal cells of hypocotyls between *GFP-2sc* and *kam1* (data not shown). Therefore, the dwarf stature of *kam1* is largely or exclusively attributable to a failure of individual cells to elongate rather than to a defect in cell division.

DISCUSSION

Interaction of KAM1/MUR3 and Actin Is Responsible for Proper Endomembrane Organization

The isolated *kam1* mutant showed abnormal actin distribution (Figures 8A and 8B). Several groups have reported that normal organization of the actin cytoskeleton is essential for cell morphogenesis and elongation in a variety of plant cell types and organs (Staiger, 2000; Baluska et al., 2001a; Dong et al., 2001; Chen et al., 2002; Ringli et al., 2002; Li et al., 2003; Mathur et al., 2003; Nishimura et al., 2003). Actin-interfering drugs, which perturb actin filaments, reduce the cell elongation of various organs, including hypocotyls and roots, and cause a dwarf stature (Baluska et al., 2001b). These phenotypes are similar to the phenotype conferred by *kam1*, which is characterized by a defect in the elongation of hypocotyl cells (Figures 9E and 9F) and dwarf stature (Figures 9A, 9C, and 9D). This fact suggests that the phenotype conferred by *kam1* is closely associated with the altered actin organization.

Many reports have also shown that the actin filaments contribute to the structural maintenance of endomembranes in plant cells. Depolymerization of actin filaments but not microtubules led to the inhibition of Golgi movement and the clustering of Golgi stacks on small islands of lamellar ER in tobacco leaves (Boevink et al., 1998; Brandizzi et al., 2002) and to the disassembly of the structures of ER tubules in Arabidopsis hypocotyls (Zheng et al., 2004). In the Arabidopsis *rhd3* mutant, actin organization is altered but cortical microtubule organization is not (Hu et al., 2003). The *rhd3* mutant is characterized by disorganization of the ER and Golgi stacks (Zheng et al., 2004), an abnormal distribution of vesicles in the subapical region, and an altered vacuolar organization in the root hairs (Galway et al., 1997). The Arabidopsis *crooked* mutant, in which the structure of actin filaments is altered, has an abnormal accumulation of some Golgi stacks at certain regions in trichomes (Mathur et al., 2003).

Although many studies have examined actin organization, no factor has yet been identified that involves the interaction between the endomembranes and actin filaments. *kam1*, which exhibits the same subcellular phenotypes described above, forms endomembrane aggregates within the cells (Figures 1 to 3). The endomembrane aggregates might be caused by the formation of aggregates of actin filaments in *kam1*. We suggest that KAM1/MUR3 plays an essential role in proper actin organization, which is known to be important for endomembrane organization and cell elongation. Although the structures of endomembranes were largely destroyed in *kam1* cells, vacuolar proteins, which include storage proteins in seeds and vacuolar proteases in vegetative tissues, were accurately transported to vacuoles and processed into their mature forms (data not shown). This finding suggests that KAM1/MUR3 is

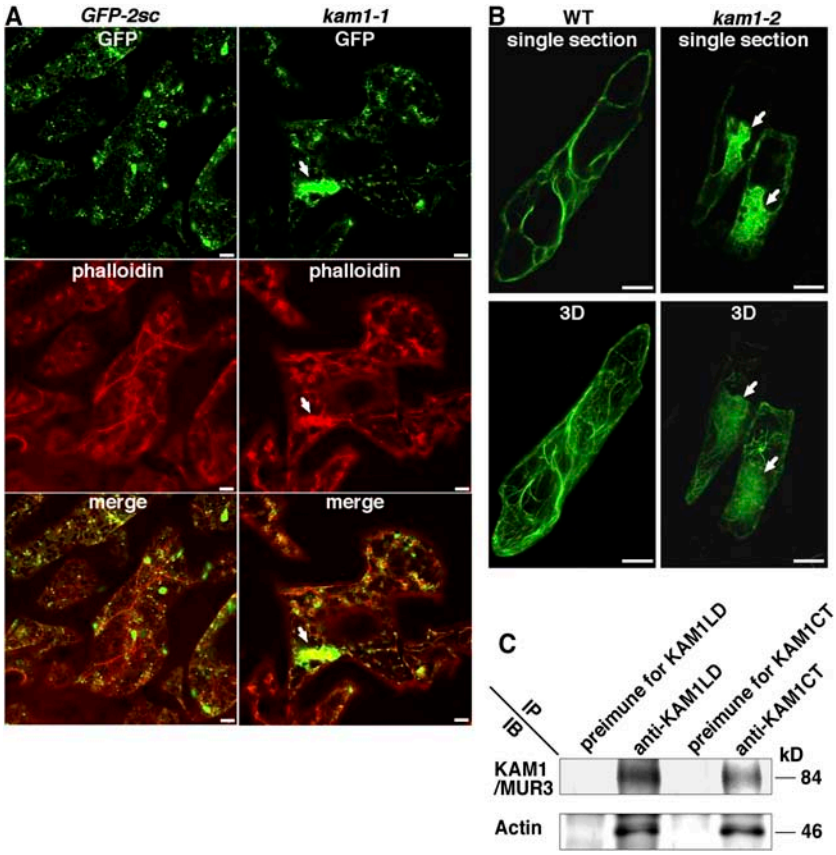

Figure 8. KAM1/MUR3 Interacts with Actin.

(A) Actin filaments in cotyledon cells of *GFP-2sc* (left panels) and *kam1-1* (right panels) were stained with Alexa Fluor 546 phalloidin. They were inspected with a confocal laser scanning microscope. Actin filaments coaggregated with GFP-fluoresced endomembranes in *kam1-1*. Arrows indicate aggregates of endomembranes and actin filaments. Bars = 5 μm.

(B) Actin filaments in stem cells of the wild type (left panels) and *kam1-2* (right panels) were visualized by transient expression of the *ABD2-GFP* construct, which encodes an actin binding domain of fimbrin protein followed by GFP. They were inspected with a confocal laser scanning microscope. The top panels show images of a single confocal section. The bottom panels show the three-dimensional structures of actin filaments that were reconstituted with sequential confocal images taken along the optical *z* axis throughout the cells. Arrows indicate aggregates of actin filaments. Bars = 10 μm.

(C) Detergent-solubilized extracts from Arabidopsis cultured cells were immunoprecipitated with anti-KAM1LD or anti-KAM1CT antibody (IP). The immunoprecipitates were subjected to immunoblot analysis with either anti-KAM1LD or anti-actin antibody. KAM1/MUR3 was coimmunoprecipitated with actin protein (IB). As negative controls, preimmune sera for each anti-KAM1 antibody were also used for the immunoprecipitation. Molecular masses are given at right.

not involved in the trafficking of proteins from the ER to the vacuoles.

KAM1/MUR3 Is a Key Component in the Golgi-Mediated Organization of Actin in Plant Cells

Two features of plant Golgi stacks that are different from those of animal and yeast are their mobility along the actin filaments and their wide distribution throughout the cytoplasm (Boevink et al., 1998; Saint-Jore et al., 2002). Therefore, it has been proposed that plant cells have novel mechanisms for the secretory pathway (Nebenfuhr and Staehelin, 2001; Neumann et al., 2003). For example, in tobacco cells, Golgi stacks move to specific sites on the surface of the ER to pick up secretory proteins (daSilva et al., 2004). This function has not been observed in yeast and animal cells.

Our findings provide another reason why plant Golgi stacks are mobile along actin filaments and distributed throughout the cytoplasm. It is possible that the plant Golgi stacks serve not only as complex carbohydrate factories and as sorting stations for the processed molecules but also as an organizer of actin filaments that run throughout cells. The finding that KAM1/MUR3 is localized on the Golgi membrane (Figures 5 and 6) implies

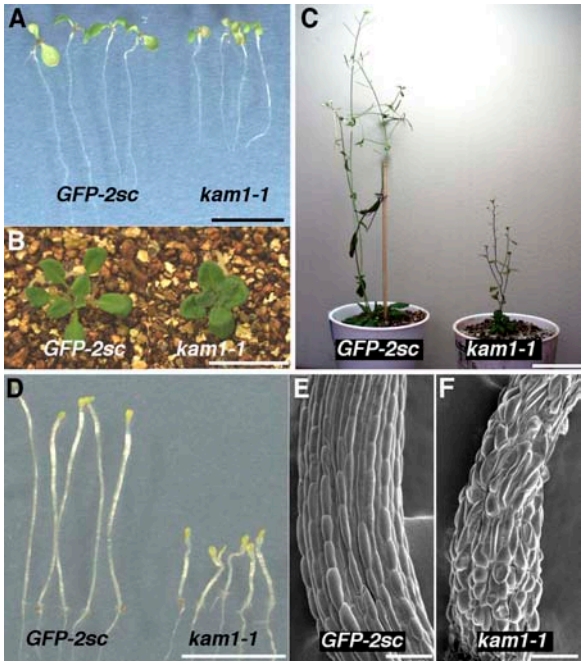

Figure 9. *kam1* Plants Exhibit a Dwarf Phenotype.

Morphological comparison at various developmental stages between *GFP-2sc* and *kam1-1* plants.
(A) Seven-day-old seedlings. Bar = 1 cm.
(B) Four-week-old plants. Bar = 1.5 cm.
(C) Six-week-old plants. Bar = 3 cm.
(D) Five-day-old seedlings grown in continuous dark. Bar = 1 cm.
(E) and **(F)** Hypocotyl cells of 5-d-old seedlings of *GFP-2sc* **(E)** and *kam1-1* **(F)** were examined with a scanning electron microscope. Bars = 100 μm.

that plant cells have a Golgi-mediated mechanism for actin organization. Although there is no evidence that actin is linked to the function of the Golgi stacks in plant cells, in mammal cells, actin binding proteins and actin regulatory proteins have been found on the Golgi membrane (Godi et al., 1998; Fucini et al., 2002; Stamnes, 2002). The overall results suggest that KAM1/MUR3 is a key component for the Golgi-mediated organization of actin in plant cells.

KAM1/MUR3 Is a Dual-Function Protein Responsible for Actin Organization and the Synthesis of Cell Wall Materials

Although KAM1/MUR3 interacts with actin (Figure 8C), how it interacts is unclear. We showed that the N-terminal domain of KAM1/MUR3 was exposed in the cytosol (Figure 5); therefore, it is possible that KAM1/MUR3 interacts with actin via the cytosolic N-terminal domain. However, the N-terminal domain has no known motifs for actin binding. An in vitro binding assay showed that the domain did not interact directly with actin (data not shown). These observations suggest that the interaction between actin and the N-terminal domain of KAM1/MUR3 requires other unidentified cytosolic factors. Profilin, which is an actin-polymerizing protein that prevents monomeric actin from forming abnormal assemblies (Baluska et al., 2001b), is a candidate for a cytosolic factor that interacts with KAM1/MUR3 on the Golgi membrane. It was reported that plant Golgi stacks move along actin filaments on the ER network using myosin motors (Boevink et al., 1998; Nebenfuhr et al., 1999). We observed that Golgi stacks were mobile along the ER network not only in wild-type leaf cells (see Supplemental Video 1 online) but also in *kam1-1* cells (see Supplemental Video 2 online). This finding suggests that KAM1/MUR3 is not involved in the Golgi stack movement driven by myosin motors and that the interaction between KAM1/MUR3 and actin filaments is independent of myosin.

On the other hand, the lumenal C-terminal domain of KAM1/MUR3 has an exostosin-like domain, which contributes to the activity of xyloglucan galactosyltransferase, an enzyme involved in the biosynthesis of the cell wall. Both the *mur3-1* and *mur3-2* mutants, each of which has a mutation in the exostosin-like domain (Madson et al., 2003), have a defect in xyloglucan galactosyltransferase activity but show normal endomembrane organization (Figure 4B). Therefore, the endomembrane organization does not require xyloglucan galactosyltransferase activity. We suggest that KAM1/MUR3 is a dual-function protein that is responsible for actin organization and the synthesis of cell wall materials. KAM1/MUR3 could interact in some way between the cytoskeleton organization and the biogenesis of the cell wall, because proper actin organization is required for the secretion of polysaccharides and enzymes from the Golgi stacks to the cell wall (Blancaflor, 2002; Hu et al., 2003).

Transgenic Arabidopsis *GFP-2sc* Plants Are an Ideal Tool for Studying Endomembrane Organization

Several groups have used GFP-based screens to isolate Arabidopsis mutants that have abnormally shaped organelles, including mitochondria (Logan et al., 2003), peroxisomes (Mano et al., 2004), vacuolar membranes (Avila et al., 2003), and ER bodies (Matsushima et al., 2003, 2004). Thus, GFP screening is a useful method for studying organelle morphology and biogenesis. However, a genetic approach to investigate the entire endomembrane system has been prevented by the lack of a simple phenotypic trait that can be used as a visual marker for the entire endomembrane system. Previously, we demonstrated that vacuole-targeted GFP (SP-GFP-2SC) can act as a visual marker for monitoring the dynamics of the entire endomembrane system in Arabidopsis cells (Tamura et al., 2003). By screening mutagenized *GFP-2sc* plants, we have identified several mutants showing abnormal endomembrane organization, which is different from the phenotype conferred by *kam1*. A phenotypic analysis of these mutants and identification of the mutated gene responsible for the abnormal phenotype should help to identify the mechanisms that control endomembrane organization, which, in turn, controls fundamental aspects of plant development.

METHODS

Plant Materials and Growth Conditions

We used wild-type plants of *Arabidopsis thaliana* (ecotypes Columbia and Landsberg *erecta*) and a transgenic plant of Arabidopsis (ecotype Columbia) that expresses SP-GFP-2SC, which is composed of a signal peptide (SP) from pumpkin (*Cucurbita pepo*) 2S albumin followed by GFP and the vacuole-targeting signal of the C-terminal 18-amino acid sequence from pumpkin 2S albumin (Tamura et al., 2003). We designated this transgenic plant *GFP-2sc*. We also used the Arabidopsis mutants *mur3-1* and *mur3-2* (Madson et al., 2003). Information about T-DNA insertion mutants, salk_127057 (*kam1-2*) and salk_141953 (*kam1-3*), was obtained from the Salk Institute Genomic Analysis Laboratory website (http://signal.salk.edu). All seeds were provided by the ABRC at Ohio State University. Surface-sterilized seeds were sown onto 0.5% Gellan Gum (Wako, Osaka, Japan) with MS medium (Wako) supplemented with B5 vitamins and 1% sucrose and were grown at 22°C under continuous light. Protoplasts were prepared from Arabidopsis cultured cells, which had been subcultured, and were incubated in medium containing MS salts, B5 vitamins, 1% (w/v) sucrose, and 0.4 M mannitol as described previously (Tamura et al., 2003).

Plasmid Construction

The *mRFP1* gene was kindly provided by R.Y. Tsien of Howard Hughes Medical Institute (Campbell et al., 2002). We amplified *mRFP* with a specific primer harboring a *Xho*I site and a specific primer harboring a *Sac*I site by PCR to produce pmRFP. The amplified DNA was inserted into the *Xho*I-*Sac*I site of pBI221 (Clontech, Palo Alto, CA) to generate mRFP/pBI221. Based on mRFP/pBI221, we constructed a chimeric gene encoding each of two modified mRFPs as follows.

The cDNAs of KAM1/MUR3 and KAM1ΔC were amplified by PCR from a cDNA library prepared from Arabidopsis roots using the primer pairs 5′-CGTCTAGAATGTTTCCAAGGGTTTCTATGA-3′ and 5′-CGCTCGAGCTGTGTCTTATCTCTCTGCTCA-3′ for KAM1/MUR3 and 5′-CGTCTAGAATGTTTCCAAGGGTTTCTATGA-3′ and 5′-CGCTCGAGGGAACTAGAATTGGCTACTGGT-3′ for KAM1ΔC. The amplified fragments were inserted into the *Xba*I-*Xho*I site of mRFP/pBI221. These chimeric genes encode the full length of KAM1/MUR3 followed by mRFP1 (KAM1-mRFP) and the N-terminal 119-amino acid sequence of KAM1/MUR3 followed by mRFP1 (KAM1ΔC-mRFP).

The chimeric gene encoding SP-mRFP-HDEL was produced by three rounds of PCR amplification as follows. First, the DNA fragment for a SP was amplified using SP-GFP (Mitsuhashi et al., 2000) as a template and a set of oligonucleotide primers, 5′-CTCGAGATGGCCAGACTCACAAGCATCATT-3′ and 5′-CATGCCGCCCATGGTGCGGTAGGCGTA-3′. Second, the mRFP-HDEL DNA fragment was amplified using pmRFP as a template and a set of oligonucleotide primers, 5′-ATGGGCGGCATGCGGGGTTCTCATCATCAT-3′ and 5′-AGATCTTCAAAGCTCATCGTGTCCTCCTCCGGCGCCGGTGGAGTGGCGGCCCTCGGCGCGCT-3′. Third, the SP-mRFP-HDEL DNA fragment was amplified using both PCR fragments as templates and a set of oligonucleotide primers, 5′-ATGGGCGGCATGCGGGGTTCTCATCATCAT-3′ and 5′-AGATCTTCAAAGCTCATCGTGTCCTCCTCCGGCGCCGGTGGAGTGGCGGCCCTCGGCGCGCT-3′. The amplified fragment SP-mRFP-HDEL was inserted into the *Xho*I-*Bgl*II site of SP-GFP-CTTP/pBI221 (Tamura et al., 2003). The chimeric gene encodes a SP and mRFP followed by a 12-amino acid sequence including an ER-retention signal, HDEL.

The DNA fragment for mRFP–peroxisome-targeting signal 1 (PTS1) was produced by PCR amplification using pmRFP as a template and the primer pair 5′-GCTCGAGATGCGGGGTTCTCATCATCATCA-3′ and 5′-GAGCTCTCACAGCTTTGACACAGGCAATTCCAAGGCTTTGAGATCGGCGCCGGTGGAGTGGCGGCCCTC-3′. This amplified fragment was inserted into the *Xho*I-*Sac*I site of pBI221. This chimeric gene encodes mRFP followed by a 12-amino acid sequence including PTS1 (Mano et al., 2002).

Transient and Stable Expression in Arabidopsis

Protoplasts from Arabidopsis cultured cells were transformed with each of the chimeric genes using polyethylene glycol as described previously (Shimada et al., 2002). Arabidopsis plants (1 to 3 weeks old) were transformed with each chimeric gene by particle bombardment as described previously (Matsushima et al., 2004). To generate transgenic Arabidopsis plants, we transformed *kam1-1* with a chimeric gene encoding KAM1-mRFP by the in planta method (Bechtold and Pelletier, 1998).

Isolation of the *kam1* Mutant

GFP-2sc seeds were mutagenized by soaking them for 16 h in 0.2 or 0.25% (v/v) methanesulfonic acid ethyl ester (Sigma-Aldrich, Tokyo, Japan) and then washed for 11 h in running water to obtain M1 seeds. The M1 seeds were grown after self-fertilization, and the M2 seeds were collected from individual M1 plants to generate the M2 lines (669 lines).

Thirty seed grains from each M2 line were grown to obtain 5- to 7-d-old seedlings. We examined each seedling with a fluorescence microscope and selected a mutant line that exhibited abnormal endomembrane structure. We named the mutant *katamari1-1* (*kam1-1*).

Map-Based Cloning of the *KAM1* Gene

The *kam1-1* homozygous mutant (ecotype Columbia) was crossed with Landsberg *erecta* wild-type plants to generate a mapping population. In the F2 generation, the *kam1-1* mutants were selected and DNA was isolated from the leaf tissues. The polymorphism between Columbia and Landsberg *erecta* was analyzed using a combination of cleaved amplified polymorphic sequence and simple sequence length polymorphism markers (Konieczny and Ausubel, 1993; Bell and Ecker, 1994) with data obtained from The Arabidopsis Information Resource (http://www.arabidopsis.org). Approximately 20 recombinant plants of the F2 progeny were screened for the *kam1* phenotype for rough mapping. The position of the *KAM1* gene was located in the middle of chromosome 2. For fine-scale mapping, DNA was isolated from 450 plants of the F2 progeny. Nucleotide sequences were determined from both strands using the ABI Prism Big Dye Terminator cycle sequence reaction kit (Applied Biosystems, Foster City, CA) and a DNA sequencer (Prism 3100; Applied Biosystems).

Specific Antibodies and Immunoblot Analysis

Two polypeptides derived from KAM1/MUR3, Ser-57 to Gln-619 (KAM1LD: lumenal domain) and Arg-542 to Gln-619 (KAM1CT: C-terminal domain), were bacterially produced and injected into an each rabbit subcutaneously with complete Freund's adjuvant. After 3 weeks, two booster injections with incomplete adjuvant were given at 7-d intervals. Two weeks after the booster injections, blood was drawn and the antibodies were prepared.

Immunoblot analysis was performed essentially as described previously (Shimada et al., 2002), except that the dilutions of the antibodies were as follows: anti-actin (1:1,000; ICN, Aurora, OH), anti-AtELP against Arabidopsis VSR1 (1:10,000) (Shimada et al., 2003), anti-BiP (1:40,000) (Hatano et al., 1997), anti-KAM1LD (1:500), anti-KAM1CT (1:500), and anti-RGP1 (Dhugga et al., 1997).

Suborganellar and Subcellular Fractionation

Ten-day-old Arabidopsis seedlings (~3 g fresh weight) were minced on ice in 10 mL of buffer A (100 mM Hepes-KOH, pH 7.5, 0.3 M sucrose, 5 mM

EGTA, 5 mM $MgCl_2$, and Complete proteinase inhibitors [Roche, Mannheim, Germany]). The homogenate was filtered through cheesecloth and centrifuged at 2000*g* for 20 min at 4°C to remove cellular debris. The supernatant was ultracentrifuged at 100,000*g* for 1 h at 4°C to obtain a microsomal pellet.

To perform suborganellar fractionation, the microsomal pellets were resuspended in 200 μL of each solution of buffer A, high salt-buffer (1 M NaCl, 100 mM Hepes-KOH, pH 7.5, 0.3 M sucrose, 5 mM EGTA, and 5 mM EDTA), alkaline buffer (0.1 M Na_2CO_3, pH 11, 0.3 M sucrose, 5 mM EGTA, and 5 mM EDTA), and Triton X-100 buffer (1% [v/v] Triton X-100, 100 mM Hepes-KOH, pH 7.5, 0.3 M sucrose, 5 mM EGTA, and 5 mM EDTA). After incubation for 10 min, these suspensions were ultracentrifuged at 100,000*g* for 1 h at 4°C to obtain supernatant and pellet fractions. Each fraction was subjected to immunoblot analysis.

To determine membrane topology of KAM1/MUR3, the microsomal pellets were resuspended in buffer A in the presence or absence of 1% (v/v) Triton X-100 and then were incubated with 10 ng/μL proteinase K (Sigma-Aldrich) for 15 min on ice. The reactions were terminated by the addition of 5 mM phenylmethylsulfonyl fluoride and then subjected to immunoblot analysis.

To perform subcellular fractionation, the microsomal pellets were resuspended in 0.7 mL of buffer A and layered directly on top of a 16-mL linear sucrose density gradient (10 to 50%, w/w). Centrifugation was performed in an SW28.1 rotor (Beckman, Palo Alto, CA) at 27,000 rpm for 13 h at 4°C, and 0.75-mL fractions were collected with a piston gradient fractionator (Towa Labo, Tokyo, Japan). Each fraction was concentrated with acetone and subjected to immunoblot analysis.

Immunoprecipitation

The cells were homogenized and solubilized in buffer (50 mM Tris-HCl, pH 7.5, 50 mM NaCl, 1% [v/v] 3-[(3-cholamidopropyl)dimethylammonio]-1-propanesulfonic acid, and Complete proteinase inhibitors) and then centrifuged at 10,000*g* for 20 min at 4°C to remove cellular debris. The extracts were incubated with each antibody for 16 h at 4°C and then incubated with Protein G–Sepharose FF (Amersham Pharmacia Biotech, Tokyo, Japan). After extensive washing, the Sepharose beads were boiled in SDS sample buffer (100 mM Tris-HCl, pH 6.8, 4% [v/v] SDS, 20% [v/v] glycerol, and 5% [v/v] 2-mercaptoethanol]. The resulting immunoprecipitates were subjected to immunoblot analysis.

DAPI Staining

Fifteen-day-old seedlings were stained with 1 μg/mL DAPI (Wako) in 3.7% (v/v) formaldehyde for 30 min.

Phalloidin Staining

The stock solution of fluorescent staining reagent used was 200 units/mL Alexa Fluor 546 phalloidin (Molecular Probes, Eugene, OR) in methanol. Seven-day-old seedlings were fixed in a fixation buffer containing 3.7% (v/v) formaldehyde, 10% (v/v) DMSO, and 0.1% (v/v) Nonidet P-40 for 1 h and then incubated with 20 units/mL Alexa Fluor 546 phalloidin for 1 h in MS medium.

Electron Microscopy

Roots from *GFP-2sc* and *kam1-1* seedlings were fixed with 4% (w/v) paraformaldehyde and 1% (v/v) glutaraldehyde in 0.05 M cacodylate buffer, pH 7.4. The tissues were then cut into slices with a razor blade and fixed for another 2 h. Procedures for electron microscopic analysis was essentially the same as those described previously (Hara-Nishimura et al., 1993). After staining, sections were examined with a transmission electron microscope (model 120WX; JEOL, Tokyo, Japan). Hypocotyls from *GFP-2sc* and *kam1-1* seedlings were examined with a scanning electron microscope (model VE-7800; Keyence, Osaka, Japan).

Confocal Laser Scanning Microscopy

The fluorescent images were inspected with a confocal laser scanning microscope (LSM510 META; Carl Zeiss, Jena, Germany) using the 488-nm line of a 40-mW Ar/Kr laser or the 544-nm line of a 1-mW He/Ne laser with either a 100 × 1.4 numerical aperture oil-immersion objective or a 40 × 0.75 numerical aperture dry objective. Image analysis was performed using LSM image examiner software (Carl Zeiss). The data were exported as eight-bit TIFF files and processed using Adobe Photoshop 5.5 (Adobe Systems, Tokyo, Japan).

Treatments with Latrunculin B, Nocodazol, and Colchicine

Stock solutions of reagents used were 5 mM latrunculin B in DMSO, 10 mM nocodazol in DMSO, and 100 mM colchicine in DMSO. Seven-day-old *GFP-2sc* seedlings were incubated in MS medium containing 15 μM latrunculin B, 10 μM nocodazol, 1 mM colchicine, and 1% (v/v) DMSO for 12 h.

ACKNOWLEDGMENTS

We are grateful to R.Y. Tsein (Howard Hughes Medical Institute) for his kind donation of mRFP plasmid, K.S. Dhugga (Pioneer Hi-Bred International) for his gift of antibody against pea RGP1, M.H. Sato (Kyoto University) for his kind donation of GFP-AVP2 plasmid, E.B. Blancaflor (Samuel Roberts Noble Foundation) for his kind donation of ABD2-GFP plasmid, H. Ueda (Kyoto University) for constructing SP-mRFP-HDEL, and E. Yoshida (Kyoto University) for her help in screening the *kam1-1* mutant. We also thank the ABRC for providing the seeds of Arabidopsis T-DNA insertion mutants (salk_127057 and salk_141953). This work was supported by Core Research for Evolutional Science and Technology of the Japan Science and Technology Corporation and by Grants-in-Aid for Scientific Research (16085203) and for 21st Century Centers of Excellence Research Kyoto University (A14) from the Ministry of Education, Culture, Sports, Science, and Technology of Japan.

Received February 18, 2005; revised March 17, 2005; accepted March 29, 2005; published April 29, 2005.

REFERENCES

Avila, E.L., Zouhar, J., Agee, A.E., Carter, D.G., Chary, S.N., and Raikhel, N.V. (2003). Tools to study plant organelle biogenesis. Plant Physiol. **133,** 1673–1676.

Baluska, F., Jasik, J., Edelmann, H.G., Salajova, T., and Volkmann, D. (2001a). Latrunculin B-induced plant dwarfism: Plant cell elongation is F-actin-dependent. Dev. Biol. **231,** 113–124.

Baluska, F., von Witsch, M., Peters, M., Hlavacka, A., and Volkmann, D. (2001b). Mastoparan alters subcellular distribution of profilin and remodels F-actin cytoskeleton in cells of maize root apices. Plant Cell Physiol. **42,** 912–922.

Bechtold, N., and Pelletier, G. (1998). *In planta Agrobacterium*-mediated transformation of adult *Arabidopsis thaliana* plants by vacuum infiltration. Methods Mol. Biol. **82,** 259–266.

Bell, C.J., and Ecker, J.R. (1994). Assignment of 30 microsatellite loci to the linkage map of *Arabidopsis*. Genomics **19,** 137–144.

Blancaflor, E.B. (2002). The cytoskeleton and gravitropism in higher plants. J. Plant Growth Regul. **21,** 120–136.

Boevink, P., Oparka, K., Cruz, S.S., Martin, B., Betteridge, A., and Hawes, C. (1998). Stacks on tracks: The plant Golgi apparatus traffics on an actin/ER network. Plant J. **15,** 441–447.

Boevink, P., Santa Cruz, S., Hawes, C., Harris, N., and Oparka, K.J. (1996). Virus-mediated delivery of the green fluorescent protein to the endoplasmic reticulum of plant cells. Plant J. **10,** 935–941.

Brandizzi, F., Snapp, E.L., Roberts, A.G., Lippincott-Schwartz, J., and Hawes, C. (2002). Membrane protein transport between the endoplasmic reticulum and the Golgi in tobacco leaves is energy dependent but cytoskeleton independent: Evidence from selective photobleaching. Plant Cell **14,** 1293–1309.

Campbell, R.E., Tour, O., Palmer, A.E., Steinbach, P.A., Baird, G.S., Zacharias, D.A., and Tsien, R.Y. (2002). A monomeric red fluorescent protein. Proc. Natl. Acad. Sci. USA **99,** 7877–7882.

Chen, C.Y., Wong, E.I., Vidali, L., Estavillo, A., Hepler, P.K., Wu, H.M., and Cheung, A.Y. (2002). The regulation of actin organization by actin-depolymerizing factor in elongating pollen tubes. Plant Cell **14,** 2175–2190.

daSilva, L.L., Snapp, E.L., Denecke, J., Lippincott-Schwartz, J., Hawes, C., and Brandizzi, F. (2004). Endoplasmic reticulum export sites and Golgi bodies behave as single mobile secretory units in plant cells. Plant Cell **16,** 1753–1771.

Dhugga, K.S., Tiwari, S.C., and Ray, P.M. (1997). A reversibly glycosylated polypeptide (RGP1) possibly involved in plant cell wall synthesis: Purification, gene cloning, and trans-Golgi localization. Proc. Natl. Acad. Sci. USA **94,** 7679–7684.

Dong, C.H., Xia, G.X., Hong, Y., Ramachandran, S., Kost, B., and Chua, N.H. (2001). ADF proteins are involved in the control of flowering and regulate F-actin organization, cell expansion, and organ growth in Arabidopsis. Plant Cell **13,** 1333–1346.

Esko, J.D., and Selleck, S.B. (2002). Order out of chaos: Assembly of ligand binding sites in heparan sulfate. Annu. Rev. Biochem. **71,** 435–471.

Fucini, R.V., Chen, J.L., Sharma, C., Kessels, M.M., and Stamnes, M. (2002). Golgi vesicle proteins are linked to the assembly of an actin complex defined by mAbp1. Mol. Biol. Cell **13,** 621–631.

Galway, M.E., Heckman, J.W., Jr., and Schiefelbein, J.W. (1997). Growth and ultrastructure of *Arabidopsis* root hairs: The rhd3 mutation alters vacuole enlargement and tip growth. Planta **201,** 209–218.

Godi, A., Santone, I., Pertile, P., Devarajan, P., Stabach, P.R., Morrow, J.S., Di Tullio, G., Polishchuk, R., Petrucci, T.C., Luini, A., and De Matteis, M.A. (1998). ADP ribosylation factor regulates spectrin binding to the Golgi complex. Proc. Natl. Acad. Sci. USA **95,** 8607–8612.

Grabski, S., De Feijter, A.W., and Schindler, M. (1993). Endoplasmic reticulum forms a dynamic continuum for lipid diffusion between contiguous soybean root cells. Plant Cell **5,** 25–38.

Hara-Nishimura, I., Takeuchi, Y., Inoue, K., and Nishimura, M. (1993). Vesicle transport and processing of the precursor to 2S albumin in pumpkin. Plant J. **4,** 793–800.

Hatano, K., Shimada, T., Hiraiwa, N., Nishimura, M., and Hara-Nishimura, I. (1997). A rapid increase in the level of binding protein (BiP) is accompanied by synthesis and degradation of storage proteins in pumpkin cotyledons. Plant Cell Physiol. **38,** 344–351.

Herman, E.M., Tague, B.W., Hoffman, L.M., and Kjemtrup, S.E. (1990). Retention of phytohemagglutinin with carboxyterminal tetrapeptide KDEL in the nuclear envelope and the endoplasmic reticulum. Planta **182,** 305–312.

Hu, Y., Zhong, R., Morrison, W.H., III, and Ye, Z.H. (2003). The *Arabidopsis* RHD3 gene is required for cell wall biosynthesis and actin organization. Planta **217,** 912–921.

Kato, T., Morita, M.T., Fukaki, H., Yamauchi, Y., Uehara, M., Niihama, M., and Tasaka, M. (2002). SGR2, a phospholipase-like protein, and ZIG/SGR4, a SNARE, are involved in the shoot gravitropism of Arabidopsis. Plant Cell **14,** 33–46.

Konieczny, A., and Ausubel, F.M. (1993). A procedure for mapping *Arabidopsis* mutations using co-dominant ecotype-specific PCR-based markers. Plant J. **4,** 403–410.

Kyte, J., and Doolittle, R.F. (1982). A simple method for displaying the hydropathic character of a protein. J. Mol. Biol. **157,** 105–132.

Li, S., Blanchoin, L., Yang, Z., and Lord, E.M. (2003). The putative Arabidopsis arp2/3 complex controls leaf cell morphogenesis. Plant Physiol. **132,** 2034–2044.

Logan, D.C., Scott, I., and Tobin, A.K. (2003). The genetic control of plant mitochondrial morphology and dynamics. Plant J. **36,** 500–509.

Madson, M., Dunand, C., Li, X., Verma, R., Vanzin, G.F., Caplan, J., Shoue, D.A., Carpita, N.C., and Reiter, W.D. (2003). The *MUR3* gene of Arabidopsis encodes a xyloglucan galactosyltransferase that is evolutionarily related to animal exostosins. Plant Cell **15,** 1662–1670.

Mano, S., Nakamori, C., Hayashi, M., Kato, A., Kondo, M., and Nishimura, M. (2002). Distribution and characterization of peroxisomes in *Arabidopsis* by visualization with GFP. Plant Cell Physiol. **43,** 331–341.

Mano, S., Nakamori, C., Kondo, M., Hayashi, M., and Nishimura, M. (2004). An *Arabidopsis* dynamin-related protein, DRP3A, controls both peroxisomal and mitochondrial division. Plant J. **38,** 487–498.

Mathur, J., Mathur, N., Kirik, V., Kernebeck, B., Srinivas, B.P., and Hulskamp, M. (2003). *Arabidopsis CROOKED* encodes for the smallest subunit of the ARP2/3 complex and controls cell shape by region specific fine F-actin formation. Development **130,** 3137–3146.

Matsushima, R., Fukao, Y., Nishimura, M., and Hara-Nishimura, I. (2004). *NAI1* gene encodes a basic-helix-loop-helix-type putative transcription factor that regulates the formation of an endoplasmic reticulum-derived structure, the ER body. Plant Cell **16,** 1536–1549.

Matsushima, R., Kondo, M., Nishimura, M., and Hara-Nishimura, I. (2003). A novel ER-derived compartment, the ER body, selectively accumulates a β-glucosidase with an ER retention signal in *Arabidopsis*. Plant J. **33,** 493–502.

Mitsuda, N., Enami, K., Nakata, M., Takeyasu, K., and Sato, M.H. (2001). Novel type *Arabidopsis thaliana* H^+-PPase is localized to the Golgi apparatus. FEBS Lett. **488,** 29–33.

Mitsuhashi, N., Shimada, T., Mano, S., Nishimura, M., and Hara-Nishimura, I. (2000). Characterization of organelles in the vacuolar-sorting pathway by visualization with GFP in tobacco BY-2 cells. Plant Cell Physiol. **41,** 993–1001.

Morita, M.T., Kato, T., Nagafusa, K., Saito, C., Ueda, T., Nakano, A., and Tasaka, M. (2002). Involvement of the vacuoles of the endodermis in the early process of shoot gravitropism in Arabidopsis. Plant Cell **14,** 47–56.

Nebenfuhr, A., and Staehelin, L.A. (2001). Mobile factories: Golgi dynamics in plant cells. Trends Plant Sci. **6,** 160–167.

Nebenfuhr, A., Gallagher, L.A., Dunahay, T.G., Frohlick, J.A., Mazurkiewicz, A.M., Meehl, J.B., and Staehelin, L.A. (1999). Stop-and-go movements of plant Golgi stacks are mediated by the acto-myosin system. Plant Physiol. **121,** 1127–1141.

Neumann, U., Brandizzi, F., and Hawes, C. (2003). Protein transport in plant cells: In and out of the Golgi. Ann. Bot. (Lond.) **92,** 167–180.

Nishimura, T., Yokota, E., Wada, T., Shimmen, T., and Okada, K. (2003). An *Arabidopsis* ACT2 dominant-negative mutation, which

disturbs F-actin polymerization, reveals its distinctive function in root development. Plant Cell Physiol. **44,** 1131–1140.

Ringli, C., Baumberger, N., Diet, A., Frey, B., and Keller, B. (2002). ACTIN2 is essential for bulge site selection and tip growth during root hair development of Arabidopsis. Plant Physiol. **129,** 1464–1472.

Rojo, E., Gillmor, C.S., Kovaleva, V., Somerville, C.R., and Raikhel, N.V. (2001). *VACUOLELESS1* is an essential gene required for vacuole formation and morphogenesis in *Arabidopsis*. Dev. Cell **1,** 303–310.

Saint-Jore, C.M., Evins, J., Batoko, H., Brandizzi, F., Moore, I., and Hawes, C. (2002). Redistribution of membrane proteins between the Golgi apparatus and endoplasmic reticulum in plants is reversible and not dependent on cytoskeletal networks. Plant J. **29,** 661–678.

Saito, C., Ueda, T., Abe, H., Wada, Y., Kuroiwa, T., Hisada, A., Furuya, M., and Nakano, A. (2002). A complex and mobile structure forms a distinct subregion within the continuous vacuolar membrane in young cotyledons of *Arabidopsis*. Plant J. **29,** 245–255.

Sato, T.K., Rehling, P., Peterson, M.R., and Emr, S.D. (2000). Class C Vps protein complex regulates vacuolar SNARE pairing and is required for vesicle docking/fusion. Mol. Cell **6,** 661–671.

Shimada, T., Fuji, K., Tamura, K., Kondo, M., Nishimura, M., and Hara-Nishimura, I. (2003). Vacuolar sorting receptor for seed storage proteins in *Arabidopsis thaliana*. Proc. Natl. Acad. Sci. USA **100,** 16095–16100.

Shimada, T., Watanabe, E., Tamura, K., Hayashi, Y., Nishimura, M., and Hara-Nishimura, I. (2002). A vacuolar sorting receptor PV72 on the membrane of vesicles that accumulate precursors of seed storage proteins (PAC vesicles). Plant Cell Physiol. **43,** 1086–1095.

Solomon, L. (1964). Hereditary multiple exostosis. Am. J. Hum. Genet. **16,** 351–363.

Staiger, C.J. (2000). Signaling to the actin cytoskeleton in plants. Annu. Rev. Plant Physiol. Plant Mol. Biol. **51,** 257–288.

Stamnes, M. (2002). Regulating the actin cytoskeleton during vesicular transport. Curr. Opin. Cell Biol. **14,** 428–433.

Surpin, M., and Raikhel, N. (2004). Traffic jams affect plant development and signal transduction. Nat. Rev. Mol. Cell Biol. **5,** 100–109.

Tamura, K., Shimada, T., Ono, E., Tanaka, Y., Nagatani, A., Higashi, S., Watanabe, M., Nishimura, M., and Hara-Nishimura, I. (2003). Why green fluorescent fusion proteins have not been observed in the vacuoles of higher plants. Plant J. **35,** 545–555.

Uemura, T., Yoshimura, S.H., Takeyasu, K., and Sato, M.H. (2002). Vacuolar membrane dynamics revealed by GFP-AtVam3 fusion protein. Genes Cells **7,** 743–753.

Vitale, A., and Denecke, J. (1999). The endoplasmic reticulum: Gateway of the secretory pathway. Plant Cell **11,** 615–628.

Wang, Y.S., Motes, C.M., Mohamalawari, D.R., and Blancaflor, E.B. (2004). Green fluorescent protein fusions to Arabidopsis fimbrin 1 for spatio-temporal imaging of F-actin dynamics in roots. Cell Motil. Cytoskeleton **59,** 79–93.

Yano, D., Sato, M., Saito, C., Sato, M.H., Morita, M.T., and Tasaka, M. (2003). A SNARE complex containing SGR3/AtVAM3 and ZIG/VTI11 in gravity-sensing cells is important for *Arabidopsis* shoot gravitropism. Proc. Natl. Acad. Sci. USA **100,** 8589–8594.

Zheng, H., Kunst, L., Hawes, C., and Moore, I. (2004). A GFP-based assay reveals a role for RHD3 in transport between the endoplasmic reticulum and Golgi apparatus. Plant J. **37,** 398–414.